JOURNAL OF BACTERIOLOGY, Mar. 2003, p. 1895–1902 Vol. 185, No. 6
0021-9193/03/$08.00+0 DOI: 10.1128/JB.185.6.1895–1902.2003

Operon Structure and Regulation of the *nos* Gene Region of *Pseudomonas stutzeri*, Encoding an ABC-Type ATPase for Maturation of Nitrous Oxide Reductase

Ulrike Honisch and Walter G. Zumft*

Lehrstuhl für Mikrobiologie, Universität Karlsruhe, D-76128 Karlsruhe, Germany

Received 31 October 2002/Accepted 18 December 2002

The synthesis of a functional nitrous oxide reductase requires an assembly apparatus for the insertion of the prosthetic copper. Part of the system is encoded by maturation genes located in *Pseudomonas stutzeri* immediately downstream of the structural gene for the enzyme. We have studied the transcriptional organization and regulation of this region and found a *nosDFYL tatE* operon structure. In addition to a putative ABC transporter, consisting of NosD, NosF, and NosY, the operon encodes a Cu chaperone, NosL, and a component of the Tat translocon, TatE. The *nosD* operon was activated in response to anaerobiosis and nitrate denitrification. The membrane-bound regulator NosR was required for operon expression; in addition, DnrD, a regulator of the Crp-Fnr family, enhanced expression under anaerobic conditions. This establishes a likely signal transduction sequence of NO → DnrD → *nosR*/NosR → *nosD* operon. DnrD-dependent expression was also observed for the *nnrS* operon (located immediately downstream of the *nosD* operon), which encodes a putative heme-Cu protein (NnrS) and a member of the short-chain dehydrogenase family (ORF247). The NosF protein, encoded within the *nosD* operon, exhibits sequence similarity to ABC-type ATPases. It was fused to the *Escherichia coli* maltose-binding protein and overexpressed in soluble form. The fusion protein was purified and shown to have ATPase activity. NosF is the first maturation factor for which a catalytic function has been demonstrated in vitro.

The multicopper enzyme nitrous oxide reductase (N_2OR) undergoes a maturation process for the insertion of its prosthetic metal (32, 39, 44, 48, 49). Several accessory proteins are required for the biosynthesis of the catalytically active enzyme, some of which are encoded by genes located downstream of the N_2OR structural gene, *nosZ*. Expression of *nosZ* is dependent on the multitopic, membrane-bound regulator NosR (10). At least three proteins, encoded by the maturation genes *nosD*, *-F*, and *-Y*, form a putative assembly complex which extends to both sides of the cytoplasmic membrane. From sequence similarity, it was inferred that *nosF* may encode an ATP/GTPase and that a step in the biosynthesis of N_2OR is energy dependent (49). A *lacZ* reporter gene fusion had been used to deduce a location in the cytoplasm for NosF (9). NosD belongs to a family of proteins with a carbohydrate binding and sugar hydrolase domain (8) whose significance is still unclear. NosY is a six-helix transmembrane protein; it is presumed that, together with NosF and periplasmic NosD, it forms an ABC-type transporter. The biosynthesis of N_2OR also involves a number of additional factors which are nonessential or can be functionally replaced by other cellular processes (44).

Catalyzed assembly of the prosthetic Cu in N_2OR seems to be obligatory for the Cu_Z center, representing the catalytic site in the form of a tetranuclear CuS cluster (6, 35), rather than for the binuclear Cu_A center, which represents the electron entry site (27). Mutational inactivation of any of the *nosDYF* maturation genes results in an enzyme without the Cu_Z center (35, 45, 48). The components of the core maturation complex have not been isolated, due to the unsolved functional role, impeding the development of proper assays. Also, information about the transcriptional organization and regulation of the maturation genes is lacking. We found that the maturation genes are organized in a polycistronic *nosDFYL tatE* operon, which is followed by the *nnrS* operon. The principal factors which regulate these operons were identified. Further, we have expressed the *nosF* gene and show with the purified protein that it is an ATPase. NosF exhibits structural similarity to the ATPase of maltose or histidine ABC transporters.

MATERIALS AND METHODS

Strains, media, and growth conditions. The *Escherichia coli* strains DH10B (Gibco BRL) and XL-1Blue (Stratagene) were used as hosts for cloning and expression, respectively. MK21, a spontaneous Sm^r mutant (47) of *Pseudomonas stutzeri* ATCC14405, was the parent strain for the following mutants: MK418 (*nosR*::Tn*5*); MK402 and MK404 (both *nosD*::Tn*5*) (49); MKR2 (*fnrA*::*kan*) (11); MRD235 (*dnrD*::*kan*) (42); and MK118 (Δ*narL*::*kan*) (20). The plasmids used in this study were BRH97 for *nnrS* promoter analysis (18); pBTE1, carrying a 1.017-kb fragment with *tatE* cloned into pBluescript II SK(+) (22); cDEN1, a pJA1 cosmid clone of a *Sau*3A genomic library with the *nos* genes (5); pMal-c2, an expression vector based on *malE* of *E. coli* under the control of p_{tac} (New England Biolabs) (29); and pNS200, a pBR325 derivative carrying the maturation genes of the *nos* gene region (49).

Strains of *P. stutzeri* were grown in a synthetic asparagine- and citrate-containing medium at 30°C. Aerobic and denitrifying cultures were established as previously described (11) unless otherwise stated. The following antibiotics were used at the indicated concentrations (in micrograms per milliliter of medium): ampicillin, 100; gentamicin, 30; kanamycin, 50; and streptomycin, 200.

Recombinant DNA techniques. Plasmid DNA was prepared by a modified alkaline cell lysis method (16). Spin columns with a silica membrane (Roche Diagnostics) were used for plasmid DNA purification and preparative isolation from agarose slabs. Recombinant plasmids were transformed into *E. coli* by electroporation (15). For DNA manipulation, we followed standard protocols (38) or the instructions for commercial products provided by the manufacturers.

* Corresponding author. Mailing address: Lehrstuhl für Mikrobiologie, Universität Karlsruhe, PF 6980, D-76128 Karlsruhe, Germany. Phone: 49-721-6080. Fax: 49-721-608 8932. E-mail: walter.zumft@bio.uka.de.

Restriction endonucleases and other enzymes were purchased from MBI Fermentas.

RNA analysis. Cell sample preparation, RNA isolation, electrophoresis, nucleic acid transfer, and hybridization were done as described previously (43), but the time for precipitation of mRNA was reduced from overnight to 3 h. The following primers were used for the amplification of digoxigenin-labeled probes for Northern blot analysis: 5′-GTATCAAGGCCAGTTCACCA-3′ and 5′-TCA TCAGGATGCCGTAGTTC-3′ (*nosD*) and 5′-TATGCGC TGCTCGCCATTC C-3′ and 5′-CGCCGATCAACGCCATCAAC-3′ (*nnrS*). The gene probe for *nosD* was amplified from the plasmid pNS200, and the probe for *nnrS* was amplified from the cosmid cDEN1. To obtain a signal from the *tatE* transcript, it was necessary to use an RNA probe. This probe was generated from plasmid pBTE1 (22), using an RNA-labeling kit (Roche Diagnostics) and the primers 5′-GTATCAGCGTCTGGCAACTCC-3′ and 5′-ctaatacgacgactcactatagggagaT CAGCTCCTGCTTGACGC-3′ (the lowercase letters indicate 5′ extension for the promoter sequence of T7 RNA polymerase). PCR-derived probes for the genes *nirS* and *narG* were prepared by the incorporation of digoxigenin-dUTP as described elsewhere (20). For membrane detection, the dioxetane derivative CDP-Star (Roche Diagnostics) was used as the chemiluminescent substrate.

The 5′ end of the *nnrS* transcript was mapped by primer extension (2). Total RNA was isolated from MK21 and MK402 which had been cultivated for 1 h under nitrate-denitrifying conditions. Reverse transcription was initiated from the 5′ γ-^{32}P-labeled primer 5′-TCGCCGATCGATAACTTGCACGGAAGG-3′, which is complementary to the coding strand at positions 9119 to 9093 (18). The nucleotide sequence was obtained by the dideoxy chain termination method using the same primer with plasmid pBRH97 as the template.

Construction of plasmid pMal4F for *nosF* expression. *nosF* was amplified by PCR from plasmid pNS200 with the primers 5′-tagacaggatccATGAACGCCGT CGAGATCCA-3′ and 5′-ttcactgtcgacTCATAGACGGCCCTCCTGAGC-3′ (the lowercase letters indicate 5′ added extensions to generate restriction sites for *Bam*HI and *Sal*I). PCR amplification was done with Fast Start *Taq* DNA polymerase (Roche Diagnostics). After restriction, the fragment was ligated in plasmid pMal-c2 in frame to the 3′ end of *malE* to give pMal4F. *malE* encodes the maltose-binding protein (MBP). The amino acids ISEFGS were added at the N terminus of NosF as a consequence of the cloning procedure. The integrity of the expression vector was verified by automatic fluorescence-based cycle sequencing using the Thermo-Sequenase cycle-sequencing kit (Amersham Biosciences) according to the instructions of the manufacturer.

Conditions for expression and purification of the NosF hybrid protein. *E. coli* strain XL-1Blue was transformed with pMal4F, selecting for blue-white screening and ampicillin resistance. The strain was cultivated on a gyratory shaker (240 rpm) at 37°C in Luria-Bertani medium containing 0.2% glucose and 100 μg of ampicillin per ml of medium. After the culture had reached an optical density at 600 nm of 0.5, IPTG (isopropyl-β-D-thiogalactopyranoside) was added to a final concentration of 0.1 mM. Growth continued for 4 h at 22°C. The cells were harvested by centrifugation, and the pellet was stored at −22°C. The frozen cells were thawed, suspended in 30 ml of chromatography buffer (50 mM Tris-HCl, pH 7.4, 200 mM NaCl), and disrupted twice in a French press at 110 MPa. After centrifugation for 20 min at 15,000 × *g*, the supernatant was applied to a 5-ml column of amylose resin (New England Biolabs) equilibrated at 4°C with the buffer described above. The column was washed with 12 volumes of buffer and eluted with 10 mM maltose in chromatography buffer. Ten 2-ml fractions were collected and analyzed for protein content. If necessary, the fractions were concentrated using a Vivaspin 50 concentrator (Sartorius). MBP-NosF could be stored on ice for up to 4 days without loss of ATPase activity.

ATPase assay. ATPase activity was determined colorimetrically using Na_2HPO_4 as the standard for following inorganic phosphate (P_i) release (7). The reaction mixture contained 37.5 to 150 μg of MBP-NosF in 30 μl of ATPase buffer (100 mM Tris-HCl, pH 8.0, 8 mM ATP). It was equilibrated for 3 min at 37°C before the reaction was started by the addition of $MgCl_2$ (final concentration, 5 mM). The reaction was stopped after 2 min by transferring the mixture to reaction tubes containing 40 μl of 7.5% sodium dodecyl sulfate (SDS) (Sigma-Aldrich).

Analytical and immunochemical techniques. SDS-polyacrylamide gel electrophoresis (PAGE) with a 10% acrylamide gel was used for protein separation. Immunochemical detection of MBP-NosF was done with anti-MBP antiserum (New England Biolabs) and protein A-horseradish peroxidase conjugate (Bio-Rad) according to the instructions of the manufacturers. Protein mass spectrometry was done with a Bruker Biflex IV instrument following in-gel trypsin digestion. Protein determination was done by the Bradford dye-binding assay. Inhibitors and nucleotides were purchased from Sigma-Aldrich; ATP and ADP were obtained from Boehringer Mannheim.

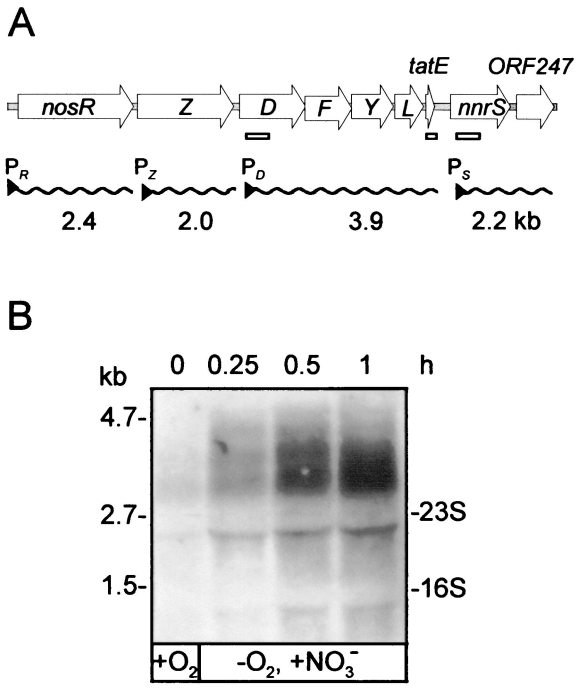

FIG. 1. Physical map of the *nos* gene region and kinetics of the *nosD* operon transcription. (A) Physical map and transcriptional organization. The wavy lines indicate transcripts from the respective promoters identified in this work or previously for *nosR* (43) and *nosZ* (10). Promoters are represented by triangles and labeled P with a qualifying subscript. The open bars show the locations and sizes of probes used in Northern hybridization. (B) Time-resolved appearance of the *nosD* transcript on shift of an aerobic culture to nitrate denitrification. Strain MK21 (representing wild-type traits) was grown aerobically (shaking frequency, 240 rpm) and probed for a *nosD* transcript by Northern blot analysis ($+O_2$). The culture was induced for denitrification by lowering the shaking frequency to 120 rpm (shift to low pO_2) and adding 1 g of sodium nitrate per liter ($-O_2$, $+NO_3^-$). The transcript was followed for 1 h after the downshift. The 0.6-kb *nosD* probe, isolation of mRNA, and conditions for hybridization were as specified in Material and Methods.

Nucleotide sequence accession numbers. EMBL databank accession numbers for the *nos* gene region are as follows: *nosR*, Z13988; *nosZ*, M22628; *nosDFY*, X53676; *nosL*, Z69589; and *tatE*, *nnrS*, and ORF274, Z73914.

RESULTS

Kinetics of *nosD* transcription on downshift to nitrate denitrification. The regulation of the maturation genes and their transcriptional organization have not yet been investigated, although the promoters of *nosR*, *nosZ*, and *nosD* were characterized previously (9). Since *nosD* is the initial gene of the maturation gene cluster (Fig. 1A), we have studied the time course of its expression on shifting cells to nitrate denitrification (Fig. 1B). In a well-aerated culture (shaking frequency, 240 rpm) of strain MK21 (representing the wild-type background), only traces of *nosD* mRNA were detected. Upon the onset of nitrate denitrification by lowering the oxygen transfer rate (the shaking frequency was reduced to 120 rpm) and adding nitrate at a final concentration of 0.1%, the amount of *nosD* transcript increased steadily. At 30 to 60 min after induction, saturation was reached. The data established the time

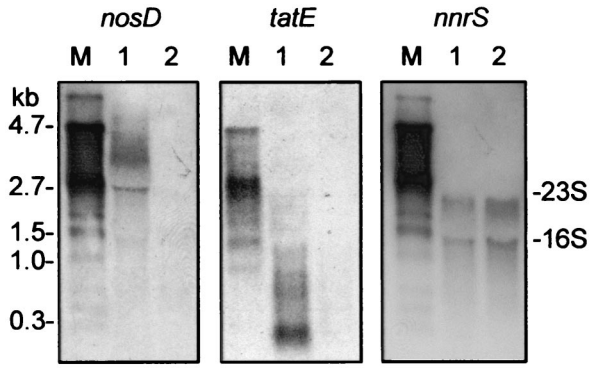

FIG. 2. Evidence for a *nosDFYL tatE* operon by mutational analysis. Total RNAs were prepared from MK21 (lanes 1) and the *nosD*::Tn*5* mutant MK402 (lanes 2). Cells were shifted to nitrate-denitrifying conditions for 60 min (shaking frequency, 120 rpm; 0.1% $NaNO_3$) prior to RNA isolation. Transcripts were detected by Northern hybridization with the DNA or RNA probes indicated at the top. The RNA molecular size marker I (M) was from Roche Diagnostics.

window for RNA sampling in subsequent induction experiments. We noticed mRNA instability on Northern blots. The size of the largest signal, ~3.9 kb, exceeded by far the size of a monocistronic *nosD* transcript and led us to investigate the formation of a polycistronic message, making use of *nosD* mutants.

Evidence for a *nosDFYL tatE* operon. To probe for the cotranscription of *nosD* with other genes, mRNA was isolated from strain MK21 and two Tn*5* insertion mutants, MK402 and MK404, 60 min after the shift from aerobic respiration to nitrate denitrification. MK402 is a *nosD* promoter mutant, whereas MK404 carries the insertion within the *nosD* coding region. The phenotype of both mutants is the synthesis of an N_2OR with only the Cu_A center metallated. Northern blot analysis was done with the probes for *nosD*, *tatE*, and *nnrS* as described in Materials and Methods. Both mutants gave the same response. Figure 2 illustrates representative results obtained with the mutant MK402. With the probes for *nosD* and *tatE*, we found transcripts in MK21 but not in MK402, whereas probing for *nnrS* resulted in a transcript of ~2.2 kb in both the wild-type background and the *nosD* mutant. The mutation in *nosD* was therefore polar on *tatE* but not on *nnrS*. This indicated a *nosDFYL tatE* operon and an independent promoter for *nnrS*. We exclude the presence of further transcriptional start sites within this operon for *nosF*, *nosY*, or *nosL*, because probing of total RNAs from MK402 and MK404 with these genes did not reveal any transcripts (data not shown).

tatE mRNA could be detected only by the use of a riboprobe (see Materials and Methods) (Fig. 2). We presume that formation of a low-mass species is related to mRNA processing or is a result of modulating the translational efficiency of the polycistronic multifunctional *nosD* operon. Processing of *tatE* is unlikely to be detectable in the 3.9-kb operon transcript because of the small size of the *tatE* gene, 171 bp.

The independent promoter for *nnrS* was confirmed by primer extension analysis (Fig. 3). We located the transcript start site at position 9194 of the published sequence (18). The promoter carries a sequence motif, CTGAT-N_4-ATCAA (positions 9230 to 9243), centered at −42.5 bp upstream of the

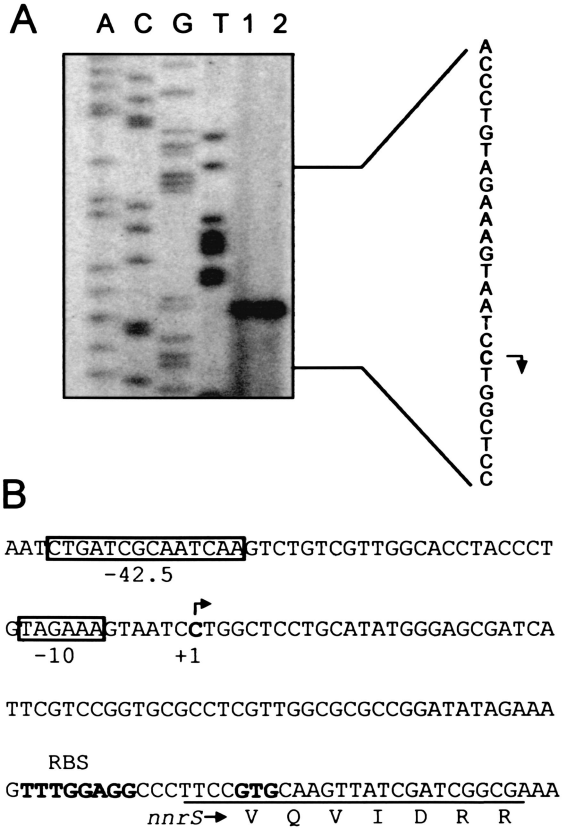

FIG. 3. Organization of the *nnrS* promoter. (A) Mapping of the 5′ terminus of the *nnrS* transcript. Primer extension reactions were done with total RNAs extracted from MK21 (lane 1) and MK402 (lane 2), which had been cultured under nitrate-denitrifying conditions. The reaction products were separated on a sequencing gel together with a sequence ladder generated with the primer indicated in panel B. The complementary sequence of the transcription initiation site is shown. (B) Features of the *nnrS* promoter. The 5′ end of the transcript is labeled +1. Putative sites for binding polymerase (−10) and DnrD (−42.5) are boxed. The oligonucleotide that was used for primer extension is underlined. The first few N-terminal amino acids of the NnrS protein are shown in one-letter code. RBS, ribosome-binding site.

transcript start site and with strong similarity to the canonical Fnr box, TTGAT-N_4-ATCAA. We assume that this regulatory motif is involved in DnrD-dependent transcription of *nnrS* (see below). DnrD and its homologues, Nnr and Dnr, are thought to bind to an Fnr-type recognition motif (for a review, see reference 46). The primer extension with RNA isolated from MK402 also corroborated the findings from Northern blot analysis with this mutant. The size determined for the *nnrS* mRNA indicated that *nnrS* was transcribed together with the gene located downstream, *orf247*.

The regulators NosR and DnrD are required for activating the *nosD* operon. The appearance of the *nosDFYL tatE* transcript in response to denitrifying conditions led to the question of which regulatory proteins are involved in the transcriptional control of this operon. NosR had been shown to be required for *nosZ* transcription (10), but it remained open whether other *nos* genes are targets of NosR. It was also shown previously that NO is a key signal for the expression of denitrifica-

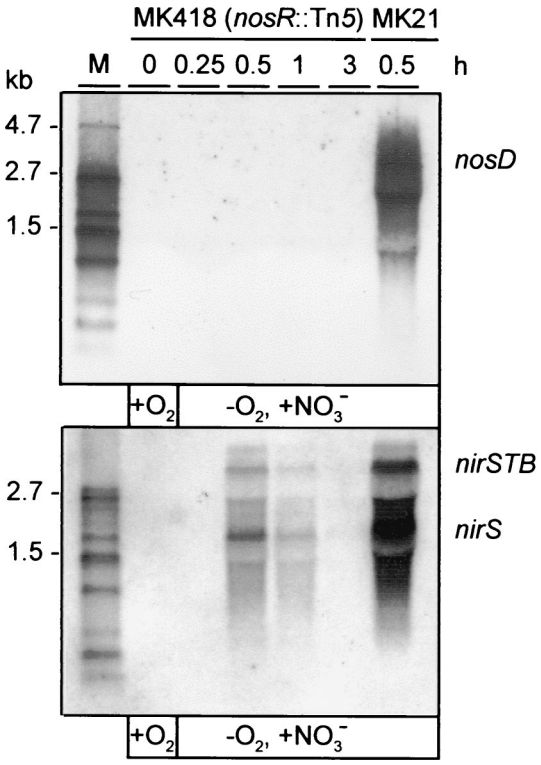

FIG. 4. Transcription of the *nosD* operon is dependent on NosR. Cells were conditioned as for Fig. 1. Total RNAs were prepared from the *nosR*::Tn*5* mutant MK418 and from MK21 and analyzed at the indicated times by Northern blotting with gene probes for *nosD* (top) and *nirS* (bottom). M, RNA marker.

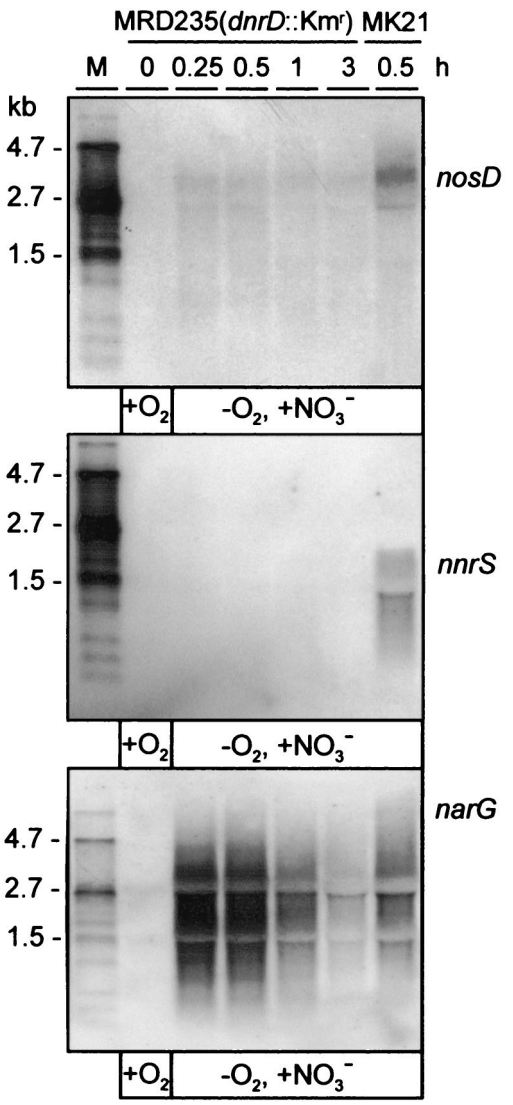

FIG. 5. DnrD enhances the expression of the *nosD* operon and is essential for *nnrS* expression. Total RNAs from MRD235 and MK21 were subjected to Northern hybridization with the gene probes for *nosD*, *nnrS*, and *narG*. The cells were conditioned as for Fig. 1. M, RNA marker.

tion genes in *P. stutzeri* and that processing of this signal involves the DnrD regulator, a member of the Crp-Fnr family (43). Therefore, we analyzed the *nosR* mutant MK418 and the *dnrD* mutant MRD235 for the presence of the *nosDFYL tatE* transcript. The absence of NosR abolished transcription of the *nosD* operon under both aerobic (i.e., the low-level transcription seen in Fig. 1B) and nitrate-denitrifying conditions (Fig. 4). To probe cells for the successful shift to the denitrifying state, the same mRNA was analyzed for transcripts from the *nirS* operon, which revealed the polycistronic and monocistronic species *nirSTB* and *nirS*, respectively (21). Activation of the *nirS* promoter is independent of NosR, and detection of the *nirS* mRNA thus proved the metabolic switch to denitrification.

The absence of DnrD also affected *nosDFYL tatE* transcription. Under denitrifying conditions, the amount of mRNA from the *nosD* operon was substantially lowered in MRD235 compared to the wild type (Fig. 5). DnrD thus acted as an enhancer of transcription under denitrifying conditions. Since the *nirS* operon is under the control of DnrD, the successful shift of MRD235 to nitrate denitrification was proven in this case by probing for the expression of the nitrate reductase operon by hybridization with *narG*.

Transcription of the *nnrS* operon was DnrD dependent and induced by nitrate-denitrifying conditions. It reached a maximum after 15 min of induction (data not shown). We observed that transcription of the *nnrS* operon under nitrate-denitrifying conditions was completely arrested in the *dnrD* mutant (Fig. 5). Other than with the *nosD* operon, no effect of NosR on transcription of the *nnrS* operon was observed; MK418 exhibited the same levels of *nnrS* mRNA as MK21.

We also probed total RNA obtained from nitrate-induced cells for *nosD* operon transcription by the *fnrA* mutant MKR2 and the *narL* mutant MRL118. These mutants are defective in the anaerobic regulator FnrA (11) and the nitrate-dependent regulator (20) of the two-component system, NarXL, respectively. Since *nosD* transcripts were found in both mutants (data not shown), it excludes these regulators from the signal transduction pathway.

Construction of the *nosF* expression vector. In an attempt to characterize biochemically the components encoded by the maturation gene cluster, we addressed the question of whether

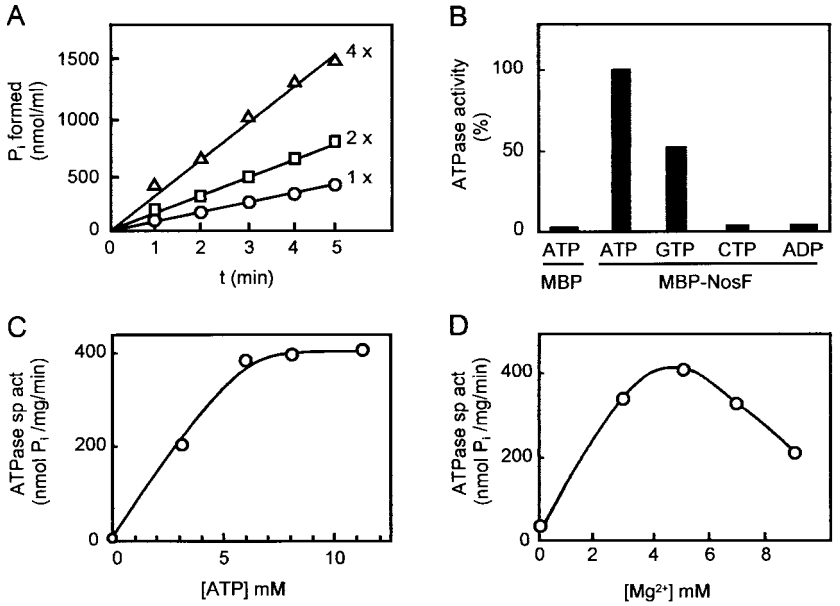

FIG. 6. Enzymatic properties of NosF. (A) NosF-catalyzed ATPase activity proceeds linearly in time and is proportional to the protein concentration. ATPase activity was assayed in 90 μl of reaction buffer; the reaction was started by the addition of $MgCl_2$; 37.5 (○), 75 (□), and 150 (△) μg of MBP-NosF were used in the assays. (B) ATP hydrolysis is specific for ATP and is due to the NosF moiety of the MBP-NosF fusion protein; 150 μg of MBP or 50 μg of MBP-NosF in 30 μl of reaction buffer and 8 mM ATP, ADP, GTP, or CTP were used. (C) Dependence of enzyme activity on ATP concentration. (D) Dependence of ATPase activity on Mg^{2+} concentration. The assays were performed as described in Materials and Methods.

the *nosF* product indeed constitutes an ATPase as predicted from sequence comparison. For this purpose, *nosF* was overexpressed in *E. coli*. To facilitate purification, we employed a fusion strategy with the MBP of *E. coli*. Insertion of *nosF* into the plasmid pMal-c2 immediately downstream of the *malE* gene generated the expression vector pMal4F (see Materials and Methods). The fusion of *nosF* to *malE* in frame and the absence of point mutations were both verified by sequencing. pMal4F resulted in the overexpression of the MBP-NosF fusion protein in the host, *E. coli* XL-1Blue.

Purification and properties of NosF. For the purification of the NosF hybrid protein, *E. coli* XL-1Blue(pMal4F) was grown at 37°C under aerobic conditions. The most favorable conditions to maximize the amount of soluble protein were induction of the cells with 0.1 mM IPTG and incubation for 4 h at 22°C. The soluble cell fraction of the induced cells exhibited a prominent band in SDS-PAGE at ~77 kDa, the mass expected for MBP-NosF. This band was absent from uninduced cells but represented by far the most abundant protein in the induced cells. The identity of this band as MBP-NosF was proven with anti-MBP antiserum by Western blot analysis and by matrix-assisted laser desorption ionization-time of flight mass spectrometry. MBP-NosF was purified from cell extract by single-step affinity chromatography on an amylose matrix. A typical preparation yielded 15 mg of MBP-NosF from a 2-liter culture. The preparation was judged to be 95% homogenous based on SDS-PAGE.

To determine whether MBP-NosF catalyzed ATP hydrolysis, we followed the release of P_i by a colorimetric assay (7). Under standard conditions, a specific activity of ~400 nmol of P_i mg of protein^{-1} min^{-1} was determined. The reaction proceeded linearly with time and was proportional to the amount of MBP-NosF (Fig. 6A). MBP has no nucleotide-binding domain and does not bind or hydrolyze ATP. Nonetheless, the possibility was considered that the ATPase activity was due to the MBP moiety, for instance, by binding traces of the MalK ATPase of the host strain. The MBP protein was expressed in strain XL-1Blue from plasmid pMal-c2 and purified identically to the procedure for MBP-NosF. No notable ATP hydrolysis was found with MBP alone (Fig. 6B). Contamination with a nonspecific phosphatase as the source of ATP hydrolysis was also excluded, since ADP as a substrate did not result in P_i release. The reaction was largely specific for ATP. GTP was hydrolyzed at a rate of ~50%, and CTP was hydrolyzed at <5% of the activity with ATP. A similar selectivity in the utilization of these nucleotides has been found for other ABC-type ATPases (1, 26, 34).

The ATPase activity of NosF was dependent on Mg^{2+} in the assay buffer, with the highest activity found in the presence of 5 mM Mg^{2+} at 8 mM ATP (Fig. 6C and D). Cu and Ca could not replace Mg. A K_m value for ATP of 3 mM and a value of 10 mM for GTP were calculated under standard conditions. The ATPase activity of NosF was moderately pH dependent in the alkaline range. The highest activity resulted between pHs 8.0 and 8.5, while at pHs 7.5 and 9.3, the activity was lowered to 80%.

The sensitivity of NosF to inhibitors was investigated. ATPase activity was measured in standard assay buffer after a 30-min incubation period on ice with the inhibitor. Both typical and atypical behaviors of NosF with respect to ABC-type ATPases were found. The sulfhydryl reagent *N*-ethylmaleimide (NEM) at 0.1 mM lowered the activity by about half, whereas

the substrate analog AMP-PNP inhibited NosF completely. Ouabain, a specific inhibitor for Na^+ and K^+ ATPases, affected ATP hydrolysis only slightly at 3 mM. Vanadate as an analog of P_i is thought to trap ADP in the transition state of ATP hydrolysis (12). Incubation with 10 mM orthovanadate reduced the ATPase activity of NosF by about half. Vanadate also impairs the ATPase activity of the purified ABC domain of the galactose importer MglA of *Salmonella enterica* serovar Typhimurium (36) and the $MalFGK_2$ (13) and $HisQMP_2$ complexes (28) but shows no effect on purified HisP (34) and MalK (19, 33). A 90% decrease in NosF-catalyzed ATPase activity was caused by 10 mM NaN_3. Azide is an inhibitor of F_0F_1 ATPases and also acts on the oleandomycin exporter OleB of *Streptomyces antibioticus* (1) and weakly on MalK (33), but not on $HisQMP_2$ (28), HisP (34), or the hemolysin exporter HlyB of *E. coli* (26).

DISCUSSION

A *nosF* knockout mutant results in an N_2OR without the Cu_Z center (49). Here, we have shown that NosF has the activity of an ATPase, and we deduce from this that Cu_Z assembly involves an energy-requiring step driven by ATP hydrolysis. The 5′ in-frame fusion of *nosF* to *malE* resulted in a soluble, overexpressed MBP-NosF hybrid. MBP has been found to be superior to other fusions in keeping passenger proteins in a soluble state (25). Further, the affected C-terminal fusion has an additional beneficial effect on protein solubility (37).

NosF shows similarity to the ATPases of ABC transporters (49). To corroborate NosF as a member of this protein family, the crystal structure of MalK (14) was used to predict the secondary structure of NosF (Fig. 7). NosF shows a high degree of correspondence with MalK in the numbers, positions, and extents of β-sheets and α-helices, in spite of a low overall sequence identity. Nearly the same correspondence was observed when the crystal structure of HisP (23) was used as the template for secondary-structure prediction. Characteristic features of ABC-type ATPases, such as the Walker motifs A and B, the ABC signature, and the switch region, are located in NosF in the same positions as in the template. MalK belongs to a special group among the ABC-type ATPases because of its C-terminal domain of 149 amino acids, which has a regulatory function and acts on MalT, the activator of *mal* gene expression (for a review, see reference 4). NosF also has a C-terminal extension of 81 amino acids, but this region has no structural correspondence to MalK (Fig. 7). No clue to the function of this NosF domain exists. A further distinguishing feature of NosF is that its ABC signature, YSKGM, does not fully correspond to the conserved region of ABC-type ATPases, which have the consensus sequence LSGGQ. Recent findings based on vanadate-catalyzed photocleavage support the notion that this motif contacts the γ-phosphate of ATP (17).

NEM is thought to inhibit the ATPase activity of ABC transporters by the covalent modification of the cysteine residue located in the P-loop (the Walker A motif). NosF lacks this residue; nevertheless, its ATPase activity was affected by NEM. The only two cysteine residues of NosF are located in and immediately behind the switch region. Thus, by modifying these residues, NEM might affect protein integrity. The switch region is thought to be involved in the signal transduction process between the transmembrane component and the ATPase of ABC transporters (40).

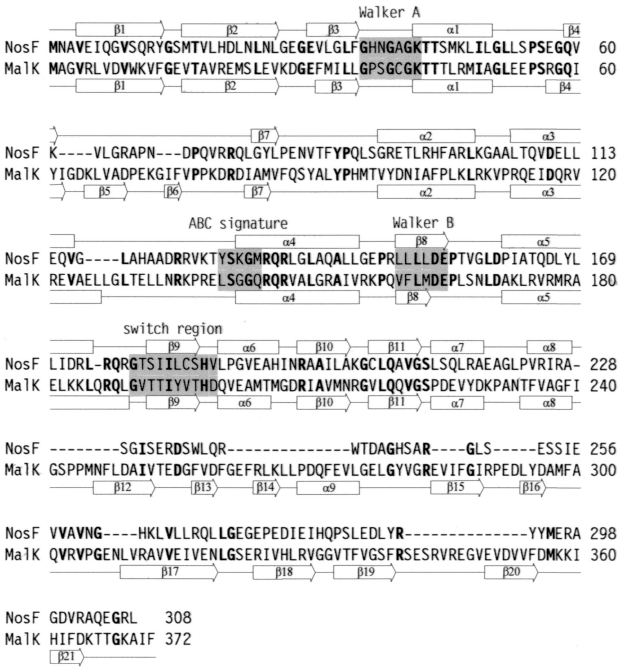

FIG. 7. Prediction of secondary structure of NosF. The protein was modeled on the crystal structure of MalK (Protein Data Bank file 1G29) using the ExPASy server of the Swiss Institute of Bioinformatics (http://www.expasy.ch). Extensions of predicted α-helices are shown by boxes; those of β-sheets are shown by arrows. The secondary structural elements of NosF are numbered according to those of MalK from *Thermococcus litoralis* (14). Distinct motifs of ABC-type ATPases are shaded. The C-terminal amino acids of NosF lack the structural elements of the C-terminal regulatory domain of MalK and could not be modeled from the template. Positionally identical residues of the two sequences are shown in boldface.

The *nosF* gene is expressed as part of the *nosDFYL tatE* operon. Although the *nosD* transcription start point is defined (9), no specific regulatory motifs are evident in the promoter region. Putative NarL binding sites for the nitrate response regulator, noted previously, appear fortuitous in light of the present results of NosR- and DnrD-dependent regulation. In aerobic cells, a small amount of N_2OR is found, i.e., *nos* genes are transcribed constitutively at a low level. Under anaerobic N_2O-respiring or nitrate-denitrifying conditions, *nos* gene expression is activated and leads to a manifold increase in cellular N_2OR content. Transcription of *nosZ* requires NosR, a multidomain transmembrane protein and putative metalloprotein (45). We have shown here that NosR also activates the transcription of the *nosD* operon. Transcription of *nosR*, in turn, is activated in response to NO and depends on the DnrD regulator, a member of the Crp-Fnr family (43). We suggest a signal transduction pathway where NO derived from nitrate denitrification leads to activation of DnrD, which results in *nosR* expression and subsequent activation of the *nosD* operon: NO → DnrD → *nosR*/NosR → *nosD*.

It remains to be established to what extent this positive control circuit involves a sequence of direct interactions. The

basal *nos* transcription allows the cell to also acquire N_2OR in the absence of DnrD on long-term exposure to anaerobic conditions. The question of an additional signal derived from the redox status or the oxygen tension remains open. No Fnr-binding sites exist in the *nosD* promoter, and a mutation in *fnrA* did not affect *nosD* transcription.

Two other functions, encoded by *nosL* and *tatE*, are part of the *nosD* operon. NosL is a Cu protein; it was tentatively assigned a metallochaperone function directed at N_2OR (32). *nosL* is consistently found as part of *nosDFY* gene clusters, emphasizing a role in the maturation process (44). TatE is a component of the Tat translocation machinery and assures complete processing and export of N_2OR (22, 44). It was unexpected to find *tatE* cotranscribed with genes for N_2OR maturation. A different stoichiometry required for the different functions encoded in polycistronic messages can be achieved by posttranscriptional control mechanisms, as exemplified for the ATPase operon of *E. coli* (30, 31) or the histidine transport operon of *S. enterica* serovar Typhimurium (41). The *nosD* operon thus may be subjected to regulation of translational efficiency or the stability of distinct mRNA segments. Probing for *tatE* has revealed a low-mass mRNA species, which is seen within this context.

The *nnrS* gene in *P. stutzeri* is adjacent to the maturation gene cluster but not part of the *nosD* operon. Nevertheless, it is expressed in response to denitrifying conditions and its transcription depends on DnrD. The *nnrS* gene product (previously called ORF396) had been predicted to be a 12-helix membrane protein (18). Recently, the homologous protein was purified from the purple bacterium *Rhodobacter sphaeroides* 2.3.4 and was shown to be a heme-Cu protein by optical and electron paramagnetic resonance spectroscopy (3). Mutational inactivation of *nnrS* resulted in an altered chemotactic behavior toward nitrate. In *R. sphaeroides*, *nnrS* is under the control of NnrR, another member of the Crp-Fnr regulator family. A putative NnrR recognition motif, CTGAT-N_4-ATCAA, is located 122 bp upstream of the translation start site of *nnrS* (3). We found in silico a striking association of *nnrS* orthologues with *nos* genes, but orthologues also exist in the nondenitrifying *Vibrio cholerae* (accession no. Q9KPN6) and *Pseudomonas putida* (http://www.tigr.org), which suggests a function for NnrS that is not limited to denitrification. Northern blot analysis of *P. stutzeri* showed that *nnrS* is transcribed with *orf247*, located downstream, resulting in a 2.2-kb transcript. The *orf247* product, composed of 247 amino acids, belongs to the family of short-chain dehydrogenases (18). Members of this family have an average of 250 residues per subunit, an N-terminal GXXXGXG coenzyme-binding pattern, and an active-site pattern of YXXXK and catalyze NAD(P)(H)-dependent oxidation-reduction reactions (24).

ACKNOWLEDGMENTS

We thank E. Härtig for providing the RNA probe, U. Schiek and S. Berker for the primer extension experiment, H. Körner for mass spectrometric analysis, and E. Schneider for a critical reading of the manuscript.

The work was supported by the Deutsche Forschungsgemeinschaft and Fonds der Chemischen Industrie.

REFERENCES

1. **Aparicio, G., A. Buche, C. Méndez, and J. A. Salas.** 1996. Characterization of the ATPase activity of the N-terminal nucleotide binding domain of an ABC transporter involved in oleandomycin secretion by *Streptomyces antibioticus*. FEMS Microbiol. Lett. **141:**157–162.
2. **Ausubel, F. M., R. Brent, R. E. Kingston, D. D. Moore, J. G. Seidman, J. A. Smith, and K. Struhl (ed.).** 1995. Current protocols in molecular biology. John Wiley & Sons, Inc., New York, N.Y.
3. **Bartnikas, T. B., Y. S. Wang, T. Bobo, A. Veselov, P. Scholes, and J. P. Shapleigh.** 2002. Characterization of a member of the NnrR regulon in *Rhodobacter sphaeroides* 2.4.3 encoding a haem-copper protein. Microbiology **148:**825–833.
4. **Boos, W., and H. Shuman.** 1998. Maltose/maltodextrin system of *Escherichia coli*: transport, metabolism, and regulation. Microbiol. Mol. Biol. Rev. **62:** 204–229.
5. **Braun, C., and W. G. Zumft.** 1992. The structural genes of the nitric oxide reductase complex from *Pseudomonas stutzeri* are part of a 30-kilobase gene cluster for denitrification. J. Bacteriol. **174:**2394–2397.
6. **Brown, K., M. Tegoni, M. Prudêncio, A. S. Pereira, S. Besson, J. J. Moura, I. Moura, and C. Cambillau.** 2000. A novel type of catalytic copper cluster in nitrous oxide reductase. Nat. Struct. Biol. **7:**191–195.
7. **Chifflet, S., A. Torriglia, R. Chiesa, and S. Tolosa.** 1988. A method for the determination of inorganic phosphate in the presence of labile organic phosphate and high concentrations of protein: application to lens ATPases. Anal. Biochem. **168:**1–4.
8. **Ciccarelli, F. D., R. R. Copley, T. Doerks, R. B. Russell, and P. Bork.** 2002. CASH-a β-helix domain widespread among carbohydrate-binding proteins. Trends Biochem. Sci. **27:**59–62.
9. **Cuypers, H., J. Berghöfer, and W. G. Zumft.** 1995. Multiple *nosZ* promoters and anaerobic expression of *nos* genes necessary for *Pseudomonas stutzeri* nitrous oxide reductase and assembly of its copper centers. Biochim. Biophys. Acta **1264:**183–190.
10. **Cuypers, H., A. Viebrock-Sambale, and W. G. Zumft.** 1992. NosR, a membrane-bound regulatory component necessary for expression of nitrous oxide reductase in denitrifying *Pseudomonas stutzeri*. J. Bacteriol. **174:**5332–5339.
11. **Cuypers, H., and W. G. Zumft.** 1993. Anaerobic control of denitrification in *Pseudomonas stutzeri* escapes mutagenesis of an *fnr*-like gene. J. Bacteriol. **175:**7236–7246.
12. **Davidson, A. L.** 2002. Mechanism of coupling of transport to hydrolysis in bacterial ATP-binding cassette transporters. J. Bacteriol. **184:**1225–1233.
13. **Davidson, A. L., S. S. Laghaeian, and D. E. Mannering.** 1996. The maltose transport system of *Escherichiacoli* displays positive cooperativity in ATP hydrolysis. J. Biol. Chem. **271:**4858–4863.
14. **Diederichs, K., J. Diez, G. Greller, C. Müller, J. Breed, C. Schnell, C. Vonrhein, W. Boos, and W. Welte.** 2000. Crystal structure of MalK, the ATPase subunit of the trehalose/maltose ABC-transporter of the archaeon *Thermococcus litoralis*. EMBO J. **19:**5951–5961.
15. **Dower, W. J., J. F. Miller, and C. W. Ragsdale.** 1988. High efficiency transformation of *E. coli* by high voltage electroporation. Nucleic Acids Res. **16:**6127–6145.
16. **Feliciello, I., and G. Chinali.** 1993. A modified alkaline lysis method for the preparation of highly purified plasmid DNA from *Escherichia coli*. Anal. Biochem. **212:**394–401.
17. **Fetsch, E. E., and A. L. Davidson.** 2002. Vanadate-catalyzed photocleavage of the signature motif of an ATP-binding cassette (ABC) transporter. Proc. Natl. Acad. Sci. USA **99:**9685–9690.
18. **Glockner, A. B., and W. G. Zumft.** 1996. Sequence analysis of an internal 9.72-kb segment from the 30-kb denitrification gene cluster of *Pseudomonas stutzeri*. Biochim. Biophys. Acta **1277:**6–12.
19. **Greller, G., R. Horlacher, J. DiRuggiero, and W. Boos.** 1999. Molecular and biochemical analysis of MalK, the ATP-hydrolyzing subunit of the trehalose/maltose transport system of the hyperthermophilic archaeon *Thermococcus litoralis*. J. Biol. Chem. **274:**20259–20264.
20. **Härtig, E., U. Schiek, K.-U. Vollack, and W. G. Zumft.** 1999. Nitrate and nitrite control of respiratory nitrate reduction in denitrifying *Pseudomonas stutzeri* by a two-component regulatory system homologous to NarXL of *Escherichia coli*. J. Bacteriol. **181:**3658–3665.
21. **Härtig, E., and W. G. Zumft.** 1999. Kinetics of *nirS* expression (cytochrome cd_1 nitrite reductase) in *Pseudomonas stutzeri* during the transition from aerobic respiration to denitrification: evidence for a denitrification-specific nitrate- and nitrite-responsive regulatory system. J. Bacteriol. **181:**161–166.
22. **Heikkilä, M. P., U. Honisch, P. Wunsch, and W. G. Zumft.** 2001. Role of the Tat transport system in nitrous oxide reductase translocation and cytochrome cd_1 biosynthesis in *Pseudomonas stutzeri*. J. Bacteriol. **183:**1663–1671.
23. **Hung, L.-W., I. X. Wang, K. Nikaido, P.-Q. Liu, G. F.-L. Ames, and S.-H. Kim.** 1998. Crystal structure of the ATP-binding subunit of an ABC transporter. Nature **396:**703–707.
24. **Jörnvall, H., J.-O. Höög, and B. Persson.** 1999. SDR and MDR: completed genome sequences show these protein families to be large, of old origin, and of complex nature. FEBS Lett. **445:**261–264.
25. **Kapust, R. B., and D. S. Waugh.** 1999. *Escherichia coli* maltose-binding protein is uncommonly effective at promoting the solubility of polypeptides to which it is fused. Protein Sci. **8:**1668–1674.
26. **Koronakis, V., C. Hughes, and E. Koronakis.** 1993. ATPase activity and

ATP/ADP-induced conformational change in the soluble domain of the bacterial protein translocator HlyB. Mol. Microbiol. **8:**1163–1175.
27. **Kroneck, P. M. H., W. A. Antholine, J. Riester, and W. G. Zumft.** 1988. The cupric site in nitrous oxide reductase contains a mixed-valence [Cu(II), Cu(I)] binuclear center: a multifrequency electron paramagnetic resonance investigation. FEBS Lett. **242:**70–74.
28. **Liu, C. E., and G. F.-L. Ames.** 1997. Characterization of transport through the periplasmic histidine permease using proteoliposomes reconstituted by dialysis. J. Biol. Chem. **272:**859–866.
29. **Maina, C. V., P. D. Riggs, A. G. Grandea, B. E. Slatko, L. S. Moran, J. A. Tagliamonte, L. A. McReynolds, and C. di Guan.** 1988. An *Escherichia coli* vector to express and purify foreign proteins by fusion to and separation from maltose-binding protein. Gene **74:**365–373.
30. **McCarthy, J. E.** 1990. Post-transcriptional control in the polycistronic operon environment: studies of the atp operon of *Escherichia coli*. Mol. Microbiol. **4:**1233–1240.
31. **McCarthy, J. E., B. Gerstel, B. Surin, U. Wiedemann, and P. Ziemke.** 1991. Differential gene expression from the *Escherichia coli* atp operon mediated by segmental differences in mRNA stability. Mol. Microbiol. **5:**2447–2458.
32. **McGuirl, M. A., J. A. Bollinger, N. Cosper, R. A. Scott, and D. M. Dooley.** 2001. Expression, purification, and characterization of NosL, a novel Cu(I) protein of the nitrous oxide reductase (*nos*) gene cluster. J. Biol. Inorg. Chem. **6:**189–195.
33. **Morbach, S., S. Tebbe, and E. Schneider.** 1993. The ATP-binding cassette (ABC) transporter for maltose/maltodextrins of *Salmonella typhimurium*. Characterization of the ATPase activity associated with the purified MalK subunit. J. Biol. Chem. **268:**18617–18621.
34. **Nikaido, K., P.-Q. Liu, and G. F.-L. Ames.** 1997. Purification and characterization of HisP, the ATP-binding subunit of a traffic ATPase (ABC transporter), the histidine permease of *Salmonella typhimurium*. Solubility, dimerization, and ATPase activity. J. Biol. Chem. **272:**27745–27752.
35. **Rasmussen, T., B. C. Berks, J. Sanders-Loehr, D. M. Dooley, W. G. Zumft, and A. J. Thomson.** 2000. The catalytic center in nitrous oxide reductase, Cu_Z, is a copper sulfide cluster. Biochemistry **39:**12753–12756.
36. **Richarme, G., A. El Yaagoubi, and M. Kohiyama.** 1993. The MglA component of the binding protein-dependent galactose transport system of *Salmonella typhimurium* is a galactose-stimulated ATPase. J. Biol. Chem. **268:** 9473–9477.
37. **Sachdev, D., and J. M. Chirgwin.** 1998. Order of fusions between bacterial and mammalian proteins can determine solubility in *Escherichia coli*. Biochem. Biophys. Res. Commun. **244:**933–937.
38. **Sambrook, J., and D. W. Russel.** 2001. Molecular cloning: a laboratory manual, 3rd ed. Cold Spring Harbor Laboratory Press, Cold Spring Harbor, N.Y.
39. **Saunders, N. F. W., J. J. Hornberg, W. N. M. Reijnders, H. V. Westerhoff, S. de Vries, and R. J. M. van Spanning.** 2000. The NosX and NirX proteins of *Paracoccus denitrificans* are functional homologues: their role in maturation of nitrous oxide reductase. J. Bacteriol. **182:**5211–5217.
40. **Speiser, D. M., and G. F.-L. Ames.** 1991. *Salmonella typhimurium* histidine periplasmic permease mutations that allow transport in the absence of histidine-binding proteins. J. Bacteriol. **173:**1444–1451.
41. **Stern, M. J., E. Prossnitz, and G. F.-L. Ames.** 1988. Role of the intercistronic region in post-transcriptional control of gene expression in the histidine transport operon of *Salmonella typhimurium*: involvement of REP sequences. Mol. Microbiol. **2:**141–152.
42. **Vollack, K.-U., E. Härtig, H. Körner, and W. G. Zumft.** 1999. Multiple transcription factors of the FNR family in denitrifying *Pseudomonas stutzeri*: characterization of four *fnr*-like genes, regulatory responses and cognate metabolic processes. Mol. Microbiol. **31:**1681–1694.
43. **Vollack, K.-U., and W. G. Zumft.** 2001. Nitric oxide signaling and transcriptional control of denitrification genes in *Pseudomonas stutzeri*. J. Bacteriol. **183:**2516–2526.
44. **Wunsch, P., M. Herb, H. Wieland, U. M. Schiek, and W. G. Zumft.** 2003. Requirements for Cu_A and Cu-S center assembly of nitrous oxide reductase deduced from complete periplasmic enzyme maturation in the nondenitrifier *Pseudomonas putida*. J. Bacteriol. **185:**887–896.
45. **Zumft, W. G.** 1997. Cell biology and molecular basis of denitrification. Microbiol. Mol. Biol. Rev. **61:**533–616.
46. **Zumft, W. G.** 2002. Nitric oxide signaling and NO dependent transcriptional control in bacterial denitrification by members of the FNR-CRP regulator family. J. Mol. Microbiol. Biotechnol. **4:**277–286.
47. **Zumft, W. G., K. Döhler, and H. Körner.** 1985. Isolation and characterization of transposon Tn*5*-induced mutants of *Pseudomonas perfectomarina* defective in nitrous oxide respiration. J. Bacteriol. **163:**918–924.
48. **Zumft, W. G., and P. M. H. Kroneck.** 1996. Metal-center assembly of the bacterial multicopper enzyme nitrous oxide reductase. Adv. Inorg. Biochem. **11:**193–221.
49. **Zumft, W. G., A. Viebrock-Sambale, and C. Braun.** 1990. Nitrous oxide reductase from denitrifying *Pseudomonas stutzeri*: genes for copper-processing and properties of the deduced products, including a new member of the family of ATP/GTP-binding proteins. Eur. J. Biochem. **192:**591–599.